# Pro-resolving and cartilage-protective actions of Resolvin D1 in inflammatory arthritis.

Lucy V. Norling[1], Sarah E. Headland[1], Jesmond Dalli[2], Hildur H. Arnardottir[2], Oliver Haworth[1], Hefin R. Jones[1], Daniel Irimia[3], Charles N. Serhan[2*] and Mauro Perretti[1*]

**Affiliations:**

[1]William Harvey Research Institute, Barts and the London School of Medicine, Queen Mary University of London, London EC1M 6BQ, UK.

[2]Center for Experimental Therapeutics and Reperfusion Injury, Harvard Institutes of Medicine, Department of Anesthesiology, Perioperative and Pain Medicine, Brigham and Women's Hospital and Harvard Medical School, Boston, MA 02115, USA.

[3]Center for Engineering in Medicine, Massachusetts General Hospital, Harvard Medical School, Shriners Hospital for Children, Boston, MA 02114, USA.

*CNS and MP share senior authorship.

To whom correspondence should be addressed: Email m.perretti@qmul.ac.uk

**Disclosure:**

C.N.S. is an inventor on patents [resolvins] assigned to BWH and licensed to Resolvyx Pharmaceuticals. C.N.S. is a scientific founder of Resolvyx Pharmaceuticals and owns equity in the company of undetermined value. C.N.S.' interests were reviewed and are managed by the Brigham and Women's Hospital and Partners HealthCare in accordance with their conflict of interest policies.

**Abstract:**

Rheumatoid arthritis (RA) is a debilitating disease characterised by persistent accumulation of leukocytes within the articular cavity and synovial tissue. Metabololipidomic profiling of arthritic joints from omega-3 supplemented mice identified elevated levels of specialized pro-resolving lipid mediators (SPM) including resolvin D1 (RvD1). Profiling of human RA synovial fluid revealed physiological levels of RvD1, which once applied to human neutrophils attenuated chemotaxis. These results prompted analyses of the anti-arthritic properties of RvD1 in a model of murine inflammatory arthritis. The stable epimer 17*R*-RvD1 (100ng/day) significantly attenuated arthritis severity, cachexia, hind-paw edema, paw leukocyte infiltration and shortened the remission interval. Metabololipidomic profiling in arthritic joints revealed 17*R*-RvD1 significantly reduced $PGE_2$ biosynthesis, whilst increasing levels of protective SPM. Molecular analyses indicated that 17*R*-RvD1 enhanced expression of genes associated with cartilage matrix synthesis, and direct intra-articular treatment induced chondroprotection. Joint protective actions of 17*R*-RvD1 were abolished in RvD1 receptor deficient mice termed *ALX/fpr2/3*$^{-/-}$. These investigations open new therapeutic avenues for inflammatory joint diseases providing mechanistic substance for the benefits of omega-3 supplementation in RA.

**Introduction:**

Rheumatoid arthritis (RA) is a chronic debilitating disease characterised by persistent synovitis, which leads to joint damage, increased disability and accelerated cardiovascular disease, and hence higher mortality (1). It is now appreciated that chronic inflammatory diseases such as arthritis may persist due to a failure of resolution responses (2). Current treatment strategies for RA aim to intervene early to consistently limit inflammation in order to maintain joint integrity (3). Accordingly, patient prognosis has dramatically improved since earlier diagnosis, along with the revolutionary advent of biologics, and treatment with disease modifying anti-rheumatics and methotrexate (4). Despite this, current expectations are that only 50% of treated patients will exhibit a reduction in disease activity score from high to a sustained level of low or, more rarely, remission (4). In addition treatment controls yet seldom repairs joint damage (5) and patients on therapies with biologics develop an increased risk of opportunistic infections (4, 6). Thus new therapeutic approaches that can counter disease chronicity and maintain joint integrity are required.

In order to circumvent the progress of acute self-resolving to persistent-chronic inflammation, the inflammatory response must be actively resolved. It is now appreciated that this process is not passive as once believed but governed by the spatiotemporal production of endogenous pro-resolving mediators for recent review see ref. (2). Uncovering these mediators, and elucidating their mechanisms of action has shed light on the promising nature of these compounds as potential therapeutics (7). Omega-3 PUFA, which are abundant in marine oils, are precursors to a new genus of bioactive lipid mediators that comprise the lipoxins, resolvins, protectins and

maresins (collectively termed specialised pro-resolving lipid mediators (SPM) (2, 7)), which exhibit potent and stereoselective protective properties such as limiting further neutrophil recruitment, enhancing containment and clearance of infections, and reducing inflammatory pain (2, 7, 8). Dietary supplementation with fish oils has proved efficacious in reducing joint pain, swollen joint count and NSAID usage in RA patients, yet there is an unmet need to determine the mechanism of action(s) of these supplements (9, 10). Thus SPM may offer a molecular mechanism and basis for the beneficial effects of omega-3 consumption in specific RA clinical endpoints (9, 10).

In the present study, we performed lipid mediator metabololipidomics on arthritic joints from mice fed a standard versus an omega-3 enriched chow to directly compare the local bioactive lipid mediator metabolome. Amongst the mediators quantified, we identified elevated levels of RvD1; that was also identified in human RA synovial fluids. When its 17*R* epimer (selected for its increased metabolic stability (11)) was administered to mice during inflammatory arthritis it significantly reduced joint inflammation. Herein, we report novel mechanisms of action of RvD1 and tested its anti-arthritic potential in an inflammatory polyarthritis model evoked by transfer of arthritogenic serum that mimics the presentation and histopathology of human RA.

**Results:**

***Dietary supplementation with omega-3 PUFA reduces arthritis and modulates the local lipid mediator profile.*** We tested whether a fish oil enriched diet could modulate the local bioactive lipid mediator metabolome and assessed the functional consequences of regulating tissue levels of these potent mediators in a neutrophillic model of arthritis triggered by transfer of arthritogenic serum (12). This model of arthritis is dependent upon IgG, FcγRs, complement, $LTB_4$ and IL-1β and is not dependent upon the adaptive immune system, yet requires a variety of innate immune cells including mast cells, macrophages and neutrophils allowing the study of the innate immune system in arthritis (12). Mice fed an omega-3 enriched chow exhibited a reduced arthritic score as compared to those on a standard chow diet (Figure 1A). We next performed lipid mediator metabololipidomics on arthritic paws. Mediators from the arachidonic acid (AA), eicosapentaenoic acid (EPA) and docosahexaenoic acid (DHA) bioactive metabolomes were identified and quantified in murine paws in accordance with published criteria including matching retention times on liquid chromatography (LC) and tandem mass spectrometry (MS/MS) fragmentation spectra (13) (Table 1).

Distinct profiles of lipid mediators were identified in naïve, arthritic and omega-3 supplemented mice undergoing arthritis, which could be separated utilising linear discriminant analysis (Figure 1B). Thus, correlations between individual lipid mediators and the three treatment groups were plotted (Figure 1C). Higher levels of maresin (MaR) 1 were found in naïve as compared to arthritic paws. Comparatively, arthritic joints were associated with higher levels of pro-inflammatory prostanoids

including thromboxane (TX) $B_2$, prostaglandin (PG) $D_2$, $PGE_2$ and $PGF_{2\alpha}$ as well as leukotriene (LT) $B_4$. Whereas the paws of arthritic mice supplemented with an omega-3 enriched diet were characterised by elevated levels of specialised pro-resolving lipid mediators (SPM) including EPA derived resolvin (Rv) E2 and RvE3 and DHA derived resolvins, of which RvD1 and RvD5 were significantly increased (Table 1, Fig 1C). These findings suggest that local production of SPM within the joints of omega-3 supplemented mice may contribute to the reduction in arthritis severity.

***Identification of SPM in human RA synovial fluids.*** We next profiled synovial fluid from human RA patients to determine the bioactive lipid mediator metabolome found within human joints (refer to Table 2 for patient demographics/treatment regimes). Using LC-MS/MS-based lipid mediator metabololipidomics we identified mediators from all three major bioactive metabolomes in human synovial fluids including DHA-derived resolvins and AA-derived eicosanoids (Figure 2A). Similarly to murine arthritic joints, AA-derived autacoids classically associated with joint pain and inflammation were detected within the synovial effusate, including $PGE_2$, $PGD_2$, $PGF_{2\alpha}$, $TXB_2$ and $LTB_4$. In these fluids we also identified the pathway marker for the protective lipoxin family 5,15-diHETE as well as the D-series resolvins, RvD1 and RvD3. All of these mediators were all identified in accordance with published criteria including matching retention times in LC (Figure 2A) and characteristic/diagnostic MS-MS fragmentation patterns (Figure 2B). Of note, the levels of these pro-resolving mediators in these inflammatory exudates were detected within physiologically

relevant concentrations (RvD1, ~31pM, bioactive concentrations: 10pM-100nM; RvD3, ~23pM bioactive concentrations 1pM-10nM) (8, 14, 15) (Table 3).

***Pro-resolving lipid mediators directly impact neutrophil migration.*** As arthritic synovial exudates contain abundant neutrophils, we utilized microfluidics chambers that provide defined spatiotemporal concentration gradients to study the role of SPM in regulating neutrophil chemotaxis in real-time and at a single cell level. We directly compared the actions of $LXA_4$, $LXB_4$, RvD1 or RvD2 on neutrophil migration towards IL-8, a classical neutrophil chemotaxis signal. Initially neutrophils were exposed to IL-8 (10nM) alone, then exposed to a set concentration (1nM) of SPM concomitantly with the IL-8 gradient over the subsequent 15 min. In the absence of IL-8 superfusion any captured PMN remained rounded and rapidly detached during the first minute of flow (Figure S1A, still images), this was also the case following exposure to SPM alone (data not shown).

Displacement and directionality were determined for each individual cell by tracking the cell centroid utilizing ImageJ software analysis. Following exposure to IL-8, cells migrated in the direction of the chemotactic gradient as seen by vertical cell trajectory paths (Figure 3A; veh), with general direction depicted by the rose plot (Figure 3B; veh). Inset in Figure 3B shows the polarized morphology of neutrophils after exposure to IL-8 plus vehicle (0.1% ethanol). In the presence of $LXA_4$, RvD1 or RvD2 neutrophils no longer responded to the chemotactic signal, and instead migrated in the direction of fluid flow (Figure 3A, B). Whilst with 1nM $LXB_4$, cells still responded to IL-8 and retained their polarized morphology. Rose plots for each

individual donor were plotted separately (Figure S1B-F). The chemotaxis index was calculated for each SPM as graphically illustrated in Figure 3C. $LXA_4$, RvD1 and RvD2 all significantly blunted PMN chemotaxis by approximately 75%. The directionality of neutrophil migration was also calculated for each SPM (see illustration Fig 3D); exposure to $LXA_4$ or RvD2 significantly reduced direct travel i.e. increased random movement. These results demonstrate that at low nanomolar concentrations, $LXA_4$, RvD1 and RvD2 each selectively impact and reduce directional migration towards IL-8. We subsequently selected RvD1, which significantly attenuated PMN chemotaxis yet had little effect on random migration to test in a neutrophilic model of arthritis.

***Treatment of mice with 17R-RvD1 treatment confers protection from inflammatory arthritis.*** RA is a progressive inflammatory disease characterized by extensive infiltration of leukocytes into the synovial cavity and articular tissues. Given that RvD1 significantly regulated human neutrophil responses and its 17*R*-epimer retains the bioactions of RvD1 while displaying higher metabolic stability (11) we next investigated the therapeutic potential of 17*R*-RvD1 (7*S*,8*R*,17*R*-trihydroxy-4*Z*,9*E*,11*E*,13*Z*,15*E*,19*Z*-docosahexaenoic acid) in protecting against leukocyte mediated join damage. Mice were injected with arthritogenic K/BxN serum and monitored over 8 days. Administration of K/BxN serum triggered robust arthritis, which rapidly developed over the first few days (Figure 4A). 17*R*-RvD1 treated mice exhibited a lower clinical score, and reduced hind paw edema compared with vehicle treated mice (Figure 4A and B). 17*R*-RvD1 also protected from the transient weight loss associated with arthritis (Figure 4C). Disease penetrance, defined as the

proportion of mice developing a clinical score greater than 1 out of a maximum 12 was 100% regardless of treatment group (Figure 4D), yet the clinical data indicates 17*R*-RvD1 significantly reduced disease severity.

In addition to the macroscopic assessment of arthritis, histological analyses were performed on knee joints to assess inflammatory infiltrate, cartilage degradation, and evidence of bone erosion. Microscopic analyses of the naïve, non-arthritic articular joint presented little evidence for leukocyte infiltration and demonstrated intact cartilage and bone. Arthritic serum provoked a marked accumulation of leukocytes within the joint as well as evident pannus formation and synovial hypertrophy as compared with naïve animals, whereas 17*R*-RvD1 treatment limited leukocyte recruitment, synovitis and pannus intrusion (Figure 4E-G, Figure S2A,B). Blinded analyses of histopathological sections revealed a significant tissue protection by 17*R*-RvD1 (Figure 4H). Levels of KC (CXCL1), a key chemokine known to drive inflammatory arthritis and promote leukocyte recruitment, were assessed (16). Plasma levels were elevated during arthritis and were significantly dampened following 17*R*-RvD1 treatment (Figure 4I). Further studies were performed to decipher which leukocytes infiltrated arthritic joints. Flow cytometric analyses identified neutrophil ($Ly6G^{hi}CD11b^{hi}$), monocyte ($Ly6C^{hi}Ly6G^{lo}$) and macrophage ($F4/80^{hi}Ly6G^{lo}$) accumulation within arthritic paws. Each of these leukocyte subtypes was significantly reduced in paws from 17*R*-RvD1 treated mice (Figure 4J-L).

Current arthritis treatment strategies aim to intervene early to reduce synovitis and prevent cartilage degradation and bone erosion (3). Hence, our interest was to

determine whether 17*R*-RvD1 would be effective at reducing the clinical signs of early experimental arthritis. Therapeutic administration of resolvins at the peak of an acute inflammatory response is known to accelerate the resolution process (17). Therefore the time taken to remit (remission interval) based on clinical score was calculated analogously to the resolution interval widely used to calculate the loss of neutrophils from an inflammatory site by 50% (17, 18). 17*R*-RvD1 was tested as a therapeutic agent after the second dosing of K/BxN serum when mice exhibited overt signs of arthritis (100ng, i.p. daily from day 4-10). Resolvin treatment limited the arthritis severity ($T_{max}$; Veh day 8, max. score 9.5 vs. 17*R*-RvD1 day 6, max. score 7) and shortened the remission interval ($R_i$: Veh 15 days, 17*R*-RvD1 9 days) (Figure 4M). This experiment demonstrates the potential of 17*R*-RvD1 as a therapeutic for limiting tissue damage in patients with early RA.

***Administration of 17R-RvD1 selectively modulates the local bioactive lipid metabolome within arthritic paws.*** Because RvD1 regulates pro-inflammatory eicosanoid biosynthesis during acute peritonitis (15), we next performed lipid mediator metabololipidomics on arthritic paws obtained 8 days after K/BxN serum administration to elucidate the potential mechanism(s) underlying 17*R*-RvD1 actions. Identification was conducted using established criteria (13), including liquid chromatography (LC) retention time and at least 6 fragment diagnostic ions in the MS/MS as illustrated for $LTB_4$ and $PGE_2$ (Figure 5A&B). In these paws, mediators from each of the three major bioactive metabolomes were identified including the following eicosanoids: $LTB_4$, $LXA_4$ and $LXB_4$ from the lipoxygenase pathway and $PGE_2$, $PGD_2$, $PGF_{2\alpha}$ and $TXB_2$ from the cyclooxygenase pathways (Figure 5C).

Multiple reaction monitoring (MRM) was utilised to quantify the individual mediator amounts. We found that 17*R*-RvD1 down-regulated production of pro-inflammatory $LTB_4$; an essential mediator required for the development of experimental arthritis (19) along with $TXB_2$ and prostaglandins $E_2$, $PGD_2$ and $PGF_{2\alpha}$ whilst activating protective $LXA_4$ and $LXB_4$ biosynthesis (Figure 5C). We also found that 17*R*-RvD1 stimulated the biosynthesis of EPA-derived SPM including the E-series resolvins RvE2 and RvE3 by ~50%. From the DHA bioactive metabolome PDx was significantly elevated in mice treated with 17*R*-RvD1. Thus, this exquisite regulation of lipid mediators may contribute to the joint protective actions following pharmacological delivery of 17*R*-RvD1.

Gene expression analysis was performed on paw tissue from arthritic mice treated with vehicle and 17*R*-RvD1 observing selective modulatory functions. A trend for down-modulation of *Il1b*, the key cytokine driving K/BxN arthritis, *Ly6g*, a marker of neutrophil influx, and *Ptsg2* (cyclooxygenase-2) essential for prostaglandin biosynthesis was detected in mice given 17*R*-RvD1. On the other hand, higher expression of *Alox15* (15-lipoxygenase) transcript, a key gene in SPM biosynthesis was detected in mice treated with 17*R*-RvD1 (Table S1). Most notably, a significant up-regulation of key genes involved in cartilage matrix synthesis was observed, namely type II collagen and aggrecan (Figure 6A). This unpredicted finding brought us to investigate the impact of 17*R*-RvD1 treatments on cartilage erosion during K/BxN arthritis. After the onset of arthritis (day 3), mice were administered 17*R*-RvD1 (100ng) directly into the knee joint along with PBS (+0.1% ethanol) into contralateral knees as control, with histological analyses being performed on day 5.

Cartilage integrity was first assessed in naïve mice, whereby the cartilage remained intact regardless of PBS or 17*R*-RvD1 treatment as measured by toluidine blue staining (Figure 6B, left panels and Figure 6C analyses). Whereas a marked reduction in toluidine blue staining on the cartilage surface was observed in PBS-injected knees of arthritic mice indicating loss of glycosaminoglycans (Figure 6B, upper right panel, white arrowheads). Remarkably, a significant protection from cartilage damage was evident in 17*R*-RvD1 treated joints as compared to paired contralateral control knees (Figure 6B, lower right panel and Figure 6C analyses).

To determine whether this was a direct effect on the chondrocytes rather than an indirect reduction of leukocyte/stromal cell-induced cartilage degradation, we took advantage of the human chondrocyte (C28/I2) micromass system to evaluate extracellular matrix (ECM) accumulation (20). Treatment of micromasses with 17*R*-RvD1 (0.1-100nM) resulted in a slight but non-significant increase in ECM accumulation (Figure 6D). When chondrocytes were stimulated with IL-1β a characteristic loss in ECM was quantified. Of note, 17*R*-RvD1 treatments significantly protected against the catabolic effects of concomitant IL-1β stimulation, leading to increased extracellular matrix deposition (Figure 6D and representative images of Alcian blue stained micromasses). As chondrocytes express the 17*R*-RvD1 receptor ALX/FPR2 (21) and 17*R*-RvD1 demonstrated direct actions on chondrocytes, we sought to determine whether this was via receptor ligation of ALX/FPR2. Addition of the specific antagonist $WRW_4$ did not have any effect on resting or IL-1β treated micromasses alone. However, the accumulative effects of 17*R*-RvD1 were reversed by the addition of $WRW_4$, suggesting this protective effect

was mediated via ALX/FPR2 (Figure 6E). Further support of ALX/FPR2 receptor dependency for the protective actions of 17*R*-RvD1 was attained in vivo by utilising mice nullified with the orthologue receptor *Fpr2/3* (22). Accordingly, we subjected these mice to arthritis and treated them daily with either vehicle (PBS + 0.1% EtOH, i.p.) or 17*R*-RvD1 (100ng, i.p.). In the absence of *Fpr2/3*, 17*R*-RvD1 no longer attenuated the clinical score (Figure 6F), swelling of hind paws or the arthritis-related manifestation of cachexia, and disease penetrance was almost identical between the two genotypes (data not shown). Histopathology of murine hind paws indicated substantial leukocyte infiltration (Fig S3A), with near maximal score (3/3) for both genotypes (Figure S3B). In summary, joint protection afforded by 17*R*-RvD1 was abolished in the absence of ALX/*Fpr2/3*.

**Discussion:**

RA is a chronic progressive autoimmune disease characterized by inflammation of the joints that manifests as swelling, pain and functional impairment. This condition can also lead to muscle wasting and osteoporosis and is associated with systemic inflammatory co-morbidities such as periodontitis and cardiovascular disease (1, 23). Although current therapeutics have revolutionized the management of RA, existing treatments aimed at limiting joint inflammation are associated with unwanted side-effects including GI disturbances and increase risk of infections. In addition, although current therapeutics may lead to significant improvement in patient prognosis by slowing or stopping disease progression, treatment rarely repairs joint damage (5).

We report here an elevated local production of SPM in arthritic joints from mice supplemented with an omega-3 enriched chow, a biochemical response that correlates with a reduction in arthritis severity. Using targeted lipid mediator metabololipidomics, we identified RvD1 as an SPM that was both elevated in arthritic paws from omega-3 supplemented mice and present in human RA synovial fluids, detected within the concentration range for physiological activities. Thus, when we tested the stable epimer 17*R*-RvD1 (11), a selective modulation of local lipid mediator biosynthesis and reduction in joint leukocyte infiltration was observed paralleled by macroscopic amelioration of arthritis severity, cachexia and hind-paw edema. We also uncovered novel tissue-protective functions of 17*R*-RvD1, such as stimulation of chondrocyte matrix production and protection from cartilage degradation. Together these findings identify 17*R*-RvD1 as a prototype for new therapeutic approaches for the treatment of arthritis.

Timely resolution of an inflammatory response is pertinent to maintain tissue homeostasis. To date, we and others have identified a number of endogenous mediators that activate resolution pathways to actively switch off inflammation, including annexin-A1 (24), gaseous mediators (e.g. hydrogen sulphide (25) and carbon monoxide (26, 27)) as well as specialised pro-resolving lipid mediators (SPM; lipoxins, resolvins, protectins and maresins (2, 7)). Dysregulated inflammation is a common determinant of many pathologies, yet only recently it was appreciated that diseases such as RA may persist, at least in part, due to a failure of resolution (28). Accordingly, essential protective roles for endogenous SPM and their receptors are indicated in experimental arthritis. Null mice lacking either 12/15-LOX (a key enzyme involved in SPM biosynthesis) or ALX/FPR2 (a high-affinity receptor for RvD1, $LXA_4$ and annexin A1), display exacerbated disease severity and tissue damage in inflammatory arthritis (29, 30). Additionally, mice nullified for 5-LOX (another key enzyme involved in SPM biosynthesis) exhibit intensified and prolonged duration of infectious arthritis (31). Furthermore, inhibiting COX-2 activity delays the resolution of collagen-induced arthritis, which can be restored with $PGE_2$-mediated $LXA_4$ production (32). Together, results from these studies emphasize the importance of endogenous SPM for the control of arthritis. Early studies demonstrated the protective effects of supplementing mice with fish oil enriched diet, with reduced susceptibility and lower severity scores when subjected to collagen-induced arthritis (33, 34). Congruently, we found that arthritic mice fed a fish oil enriched diet displayed attenuated arthritis that was associated with a reduction in pro-inflammatory lipid mediator levels and an enhanced biosynthesis of omega-3-derived SPM.

Enzymes of the SPM biosynthetic pathway as well as the RvD1 receptor are expressed in the rheumatoid synovium. Compared to OA synovia, elevated levels of 5- and 15-LOX as well as ALX/FPR2 are detected in synovial tissue of RA patients (35, 36). In the present study, we identified both RvD1 and RvD3 along with the lipoxin pathway marker 5,15-diHETE in synovial fluids from RA patients. These results add to the recent identification of RvD5, MaR1 and $LXA_4$ within synovial fluid (37). From these findings, we propose that metabololipidomic profiling can assist in RA patient stratification with the definition of lipid mediator profiles associated with specific cohorts and in the assignment of precision medical treatments and personalized RA patient care.

Aberrant infiltration of immune cells into the joint and the subsequent destruction of bone and cartilage drive loss of function. During active phases of RA, neutrophils present within synovial fluids contribute to disease pathogenesis via release of cytotoxic enzymes and reactive oxygen species (38). We previously reported that RvD1 (0.1-100nM) significantly dampened neutrophil recruitment to TNF-α stimulated endothelium (39), a pivotal cytokine that drives RA (6). Using microfluidics chambers to study bioactions at the single cell level under flow of continuous chemokine gradients, we observed potent actions of RvD1 at low nanomolar concentrations, blunting directed neutrophil locomotion. Thus, we utilized the K/BxN serum transfer model of arthritis to test the efficacy of the stable epimer 17*R*-RvD1. In this model of symmetric polyarthritis, daily treatment with 17*R*-RvD1 preserved joint integrity and lessened the histopathology of arthritis, with reduced

synovitis and pannus intrusion, and overall leukocyte infiltration. We previously demonstrated that 17*R*-RvD1 enriched nanoparticles limit leukocyte recruitment into the inflamed temporomandibular joint (40). Our current results emphasize the protective actions of 17*R*-RvD1 in limiting joint inflammation.

It is known that a lipid-cytokine-chemokine cascade drives neutrophil recruitment during experimental arthritis (16). Mechanistically, we found that administration of 17*R*-RvD1 down-regulated *Ptsg2* and elevated *Alox15* gene expression resulting in the selective modulation of the local lipid mediator metabolome. We measured reduced $LTB_4$ and prostaglandin levels that contribute to the pain and perpetuation of joint inflammation and identified select regulation of SPM levels that may contribute to the protective effects afforded by 17*R*-RvD1 administration. We also determined that 17*R*-RvD1 reduced systemic KC (CXCL1) levels, a principal chemokine that recruits neutrophils, and down-regulated *Il1b* transcripts, a key cytokine that amplifies arthritis. The main cellular source of this cytokine in this experimental model of arthritis is neutrophils (16) and correspondingly, we observed a reduction in neutrophil *Ly6g* transcripts. The anti-arthritic actions of 17*R*-RvD1 were lost in *Fpr2/3* null mice, reiterating this essential signaling pathway for RvD1 in murine inflammation (15, 41).

Once damaged, articular cartilage has limited intrinsic capability to self-repair. Importantly, we uncovered unique tissue protective functions of 17*R*-RvD1 in maintaining cartilage integrity during inflammatory arthritis. Chondrocytes were identified as target cells for the protective actions of RvD1, stimulating ECM

deposition. We provide evidence that 17*R*-RvD1 protects chondrocytes from IL-1β-induced degradation via direct ALX/FPR2 receptor ligation. This finding complements the array of known functions that pro-resolving mediators exert to repair injured tissue in the context of wound healing (42), tissue regeneration (43, 44) and restitution of gut epithelial barrier function (45). Our results indicate that mediators of resolution could be modeled to repair cartilage if, and when, their receptor target is presented on the chondrocyte. Recent work indicate that ALX/FPR2 is expressed by human chondrocytes and surface expression is upregulated in catabolic settings, like those evoked with IL-1β (21).

The results we present here using synthetic RvD1 as a prototype therapeutic tool from the SPM portfolio, a choice dictated by detection of this bioactive mediator in mouse and human joints, opens the opportunity to exploit this line of research for innovative therapeutic strategies in RA that combine potent anti-inflammatory with tissue-protective properties. Modeling RvD1 analogues or agonists at its receptor provide another avenue for therapeutic development (24). It is important to point out the prediction that compared to current therapeutic options; RvD1 and in general SPM-based therapies will be beneficial in multiple respects. Firstly, SPM do not provoke immune suppression (a major side effect associated with biologics e.g. anti-TNF therapy (6)) and rather stimulate host phagocyte functions to enhance phagocytosis and killing of microorganisms (8, 46, 47). Secondly, SPM exert bone-sparing properties (a major secondary effect associated with long-term glucocorticoid therapy is bone loss). In the context of experimental periodontitis RvE1 prevents alveolar bone loss (48), accelerates bone regeneration (43) and inhibits osteoclast maturation

and bone resorption (49). Additionally, parathyroid hormone stimulates RvD1 and RvD2 to enhance macrophage efferocytosis of apoptotic osteoblasts highlighting a role for SPM in bone homeostasis (50). Thirdly, SPM are potent analgesics (51), and relevantly 17*R*-RvD1 is anti-hyperalgesic in a model of arthritic pain (52). Finally, with the present study, we demonstrate novel chondroprotective functions of SPM, combating catabolic stimulation and promoting direct anabolic responses enabling protection from cartilage degradation during inflammatory arthritis.

In summary, we provide new mechanisms underlying the anti-arthritic properties evoked by omega-3 consumption in arthritis (10) and focus on a specific omega-3 derived SPM, namely RvD1 and its stable epimer 17*R*-RvD1, to establish proof-of-concept for the validity of this approach. We defined novel bioactions for this pro-resolving endogenous lipid mediator in the context of joint inflammation and chondroprotection. Together, these results give the foundation for the development of innovative therapeutic strategies to avert joint destruction during RA with limited side effects, ultimately for the benefit of the patients.

**Methods:**

**Animals**

Male 12-week old, ~30g, C57Bl/6 (Charles River, Kent) or *Fpr2/3* (ALX) null mice (generated on a C57Bl/6 background as described (22), and back-backcrossed 10 times) were maintained on a standard chow pellet diet and had access to water *ad libitum*, with a 12-hour light-dark cycle. For omega-3 diet enrichment studies, mice were maintained on a CRM (P) plus 10% salmon oil or standard CRM (P) chow (Special diet services, LBS Biotech) 3 weeks prior to and throughout the duration of experiments.

**Real-time neutrophil chemotaxis using microfluidics chambers**

Microfluidics chambers were engineered for testing the actions of bioactive lipid mediators on the chemotactic behaviour of human neutrophils as described previously (53). The main channel for assessing neutrophil chemotactic behaviour was modified by physical adsorption of P-selectin (50μg/mL, R&D Systems) and ICAM-1 (10μg/mL, R&D Systems) for 30 mins, followed by blocking with 2% human serum albumin (HSA, Sigma-Aldrich) in Hanks' balanced salt buffer (HBSS, Sigma-Aldrich) immediately before use. Steady-state gradients of IL-8 (0–10nM, R&D Systems) were formed in the two gradient generators connected to the main channel, one containing vehicle (0.1% ethanol) and the other containing an overlaying uniform concentration (1nM) of the specialized pro-resolving lipid mediator for testing (Lipoxin $A_4$, $B_4$, Resolvin D1 or D2, Cayman chemicals). Approximately 10μL of capillary blood was then collected from healthy volunteers using a BD genie lancet (Becton Dickinson), and diluted 1:10 with HBSS, 0.2% HSA. Neutrophils were

captured from flowing blood over ~3 min, and the first valve opened for infusion of the IL-8 gradient (fluid flow removed the majority of RBC and other cells that were not tethered to the coated chamber) allowing direct monitoring of neutrophils captured on the chamber surface. After 15 min, the gradient was switched to the second gradient generator containing a uniform concentration of the SPM combined with 10nM IL-8 gradient. Neutrophil migration in the chemokine gradient and their response(s) to addition of different SPM were recorded every 6 sec, over a 30 min period with a digital camera and Image Pro Plus software. Cell migration was analyzed using the cell-tracking function in ImageJ software, and tracks analyzed utilizing Ibidi Chemotaxis and Migration Tool. Only cells that started and remained within the field of view over the entire course of video capture were analysed. At least 20 cells were tracked per donor, with 3-4 donors per test compound.

**K/BxN serum transfer model of inflammatory arthritis**

K/BxN serum was generated in house by breeding NOD/Shiltj mice (Charles River, Italy) with KRN transgenic mice (kind gift from Dr. Mohini Gray, Edinburgh University, Edinburgh); the subsequent offspring (K/BxN mice) express both the T cell receptor (TCR) transgene KRN and the MHC class II molecule Ag7 and spontaneously develop a severe inflammatory arthritis. Serum was collected from K/BxN mice at 10 weeks of age, which causes a similar arthritis when transferred to recipient mice due to autoantibodies recognizing glucose-6-phosphate isomerase (GPI) depositing on the cartilage surface. Serum transfer induced arthritis was performed by intraperitoneal injection of 100μl of arthritogenic serum on days 0 and 2 in WT or *ALX/Fpr2/3* null mice. Disease was monitored by assessing the clinical

score (maximum 12 points per animal, 3 per limb with the following scoring system 0, no evidence of inflammation; 1, inflammation in one of the following aspects: individual phalanges joints, localized wrist/ankle or swelling on surface of paw; 2, inflammation on two aspects of paw; 3, major swelling on all aspects of paw). Paw edema was assessed by water displacement plethysmometry (Ugo Basile, Milan, Italy). Mice were weighed daily for signs of cachexia. For prophylactic treatment regime, WT mice were administered vehicle (0.1% EtOH) or 17*R*-RvD1 (100ng) in 100µl of saline i.p. daily (from day 0, 5min prior to arthritogenic serum administration). For therapeutic treatment protocol, WT mice were administered vehicle (0.1% EtOH) or 17*R*-RvD1 (100ng) in 100µl of saline i.p. daily following overt signs of arthritis (day 4) over a 7 day period. The arthritis remission interval was calculated based on arthritic score and calculated by analogy to the resolution indices widely used to calculate the loss of neutrophils from an inflammatory site (17, 18). At the end of experiments blood was collected via cardiac puncture into heparinized syringes, and centrifuged to obtain platelet-free plasma. For intra-articular treatments, WT mice were administered K/BxN serum on days 0 and 2 (100µl, i.p.) and were treated locally on day 3 with vehicle (left knee, 5µl PBS containing 0.1% EtOH) or 17*R*-RvD1 (right knee; 5µl, 100ng 17*R*-RvD1) and joints were harvested for histological analysis on day 5.

**Molecular analyses**

Arthritic ankle joints were collected on day 8 and stored in RNAlater at -80°C prior to homogenising using Precellys ceramic beads (Bertin Technologies, France). RNA was extracted using RNeasy Plus mini kit (Qiagen) and genomic DNA contamination

eliminated with Turbo DNA-free kit (Applied Biosystems, USA). Complementary DNA was synthesized using SuperScriptIII reverse transcriptase and OligoDt primers (Invitrogen). Quantitative real-time PCR was performed using QuantiTect primers (Qiagen) and ABI Prism 7900 sequence detector system (Applied Biosystems). Relative expression values were calculated following normalization to endogenous housekeeping gene *Rpl32* and using the $2^{-(\Delta\Delta Ct)}$ method normalized to a naive mouse (calibrator sample).

**Flow cytometry**

Leukocytes were isolated from arthritic paws following tissue digestion. Briefly, paws were collected after 8 days of arthritis, skin carefully removed and digestion buffer added (collagenase D (Roche, UK; 0.5μg/ml) and DNAse (Sigma, UK; 40μg/ml) in serum free RPMI). Paws were incubated at 37°C with gentle agitation and liberated cells collected via a 70μm cell-strainer, and kept on ice. Another 15ml of digestion buffer was added to the paws and incubated for a further 30 min. Liberated cells were centrifuged at 400*g* for 10min and re-suspended in PBS for counting. Leukocytes were first stained with Zombie NIR™ (Roche, UK; 1:500, 20min, 4°C) to identify live cells, and distinct leukocyte subtypes were identified using the following antibodies from ebioscience: CD45 (25μg/ml, clone 30-F11), CD11b (0.2μg/ml, clone M1/70), Ly6G (25μg/ml, clone RB6-8CS), Ly6C (0.4μg/ml, clone HK1.4) and F4/80 (10μg/ml, clone BM8). Samples were analysed using an LSR Fortessa flow cytometer and FlowJo software (Tree Star Inc.).

**Histology**

Joints were decalcified and paraffin embedded. Sections (8μm) were stained with haematoxylin & eosin or 1% aqueous toluidine blue and standard light microscopy was used to determine the degree of leukocyte infiltration/synovitis/pannus formation, bone erosion and cartilage damage which were each graded from 0 (no disease) to 3 (severe); max. 9 by two blinded examiners. Cartilage integrity was calculated from percentage area of cartilage stained with toluidine blue using thresholds applied with ImageJ software.

**Determination of plasma KC (CXCL1) levels**

Mice were sacrificed on day 8 following induction of arthritis, blood was collected via cardiac puncture into heparinized syringes, and centrifuged to obtain platelet-free plasma. KC (CXCL1) values were determined by ELISA.

**Targeted LC-MS/MS-based lipidomics of arthritic paws and synovial fluids.**

Paws were collected and immediately transferred to liquid nitrogen prior to homogenization in 1ml ice cold MeOH containing deuterated internal standards ($d_4$-$LTB_4$, $d_8$-5S-HETE, $d_4$-$PGE_2$, $d_5$-$LXA_4$ and $d_5$-$LTC_4$, 500pg each) and homogenized using a glass dounce. Synovial fluid (0.5mL) from RA patients (DXBiosamples, city, state, country) were placed in 1 mL ice cold MeOH containing deuterated internal standards ($d_4$-$LTB_4$, $d_8$-5S-HETE, $d_4$-$PGE_2$, $d_5$-$LXA_4$ and $d_5$-RvD2, 500pg each). All samples were kept at -20 ºC for 45 min to allow for protein precipitation and subjected to solid phase extraction as in (13). Methyl formate fractions were then brought to dryness using a TurboVap LP (Biotage) and products suspended in water-methanol (50:50 vol:vol) for LC-MS-MS. A Shimadzu LC-20AD HPLC and a

Shimadzu SIL-20AC autoinjector (Shimadzu, Kyoto, Japan), paired with a QTrap 6500 (ABSciex, Framingham, MA) was utilized and operated as described (13). To monitor each LM and respective pathways, an MRM method was developed with diagnostic ion fragments and identification using recently published criteria (13), including matching retention time (RT) to synthetic and authentic materials and at least six diagnostic ions for each LM. Calibration curves were obtained for each using authentic compound mixtures and deuterium labeled LM at 3.12, 6.25, 12.5, 25, 50, 100, and 200 pg. Linear calibration curves were obtained for each LM, which gave $r^2$ values of 0.98 – 0.99.

**Chondrocyte Micromass Assay**

The human chondrocyte cell line C28/I2 (kind gift from Dr Mary Goldring, Cornell Medical College, New York (54)) was utilized for micromass assays as described previously (20). Micromasses were stimulated with or without IL-1β (30ng/ml) alone or in combination with 17*R*-RvD1 (0.1-100nM) for 24h and extracellular matrix accumulation (ECM) was calculated following staining with Alcian blue as reported (21). Briefly, micromasses were fixed (4% glutaraldehyde, 15 min) acidified with HCl and stained with Alcian Blue 8GS overnight before dye extraction with guanidine hydrochloride (200µl, 6M). Absorbance of extracted dye was measured at 620nm using a Multiskan Bichromatic 348 spectrophotometer and normalized to DNA content using SYBRgreen dye (excitation 485nm and emission 535nm) with a TECAN M200 spectrophotometer (Tecan, Mannedorf, Switzerland). These values were used to generate extracellular matrix accumulation concentrations; and are expressed as percentage change from control micromasses. In some experiments, the

FPR2/ALX receptor antagonist $WRW_4$ (10μM) was added to micromasses 10 min prior to 17*R*-RvD1 addition and ECM accumulation evaluated after 24h.

**Statistics**

Statistical analyses were performed with mean ± SEM, where *n* is the biological replicate (individual mice or human donors). Data were analysed using either two-tailed paired or unpaired Student's t-test, one-way ANOVA with appropriate post hoc analysis, Mann-Whitney t-test or 2-way ANOVA with repeated measures where appropriate. Analyses were performed using GraphPad Prism, in all cases, $P<0.05$ was considered significant. Multivariate analysis of arthritis metabololipidomics was performed using linear discriminant analysis, where bioactive lipid mediator predictors were entered simultaneously to the model (carried out in SPSS 23; IBM, New York).

**Study approval:** Human peripheral blood was collected according to a protocol approved by Barts and the London Research Ethics Committee, London, United Kingdom (QMREC 2014:61), written informed consent was received from participants prior to inclusion in the study according to the declaration of Helsinki. All animal experiments were approved and performed under the guidelines of the Ethical Committee for the Use of Animals, Barts and The London School of Medicine and in accordance with the UK Home Office regulations (Guidance on the Operation of Animals, Scientific Procedures Act, 1986).

**Author contributions:** L.V.N. designed and performed experiments, analyzed data, wrote manuscript. S.E.H. performed experiments, analyzed data. J.D. and H.H.A analyzed metabololipidomics data. H.R.J. analyzed data, performed statistical analyses. O.H. assisted with flow cytometry analyses. D.I. provided unique tools for leukocyte chemotaxis. C.N.S. and M.P. provided conceptual expertise and contributed to manuscript preparation.

**Acknowledgements:** This work was funded by the Arthritis Research UK (Career Development Fellowship 19909 to L.V.N.) and Wellcome Trust Programme grant 086867/Z/08/Z to M.P. S.E.H is supported by an Arthritis Research UK foundation Fellowship 20842. J.D. was funded by a Sir Henry Dale Fellowship jointly funded by the Wellcome Trust and the Royal Society (Grant number 107613/Z/15/Z). This work forms part of the research themes contributing to the translational research portfolio of Barts and the London Cardiovascular Biomedical Research Unit, which is supported and funded by the National Institutes of Health Research. C.N.S. and work carried out in the CET&RI laboratories at BWH are supported by the National Institutes of Health (grant P01GM095467).

**References:**


1. Bacon, P.A., and Townend, J.N. Nails in the coffin: increasing evidence for the role of rheumatic disease in the cardiovascular mortality of rheumatoid arthritis. *Arthritis Rheum*. 2001;44(12):2707-2710.
2. Buckley, C.D., Gilroy, D.W., and Serhan, C.N. Proresolving lipid mediators and mechanisms in the resolution of acute inflammation. *Immunity*. 2014;40(3):315-327.
3. Raza, K., Buckley, C.E., Salmon, M., and Buckley, C.D. Treating very early rheumatoid arthritis. *Best Pract Res Clin Rheumatol*. 2006;20(5):849-863.
4. Feldmann, M., and Maini, R.N. Perspectives From Masters in Rheumatology and Autoimmunity: Can We Get Closer to a Cure for Rheumatoid Arthritis? *Arthritis Rheumatol*. 2015;67(9):2283-2291.
5. Klarenbeek, N.B., Guler-Yuksel, M., van der Kooij, S.M., Han, K.H., Ronday, H.K., Kerstens, P.J., Seys, P.E., Huizinga, T.W., Dijkmans, B.A., and Allaart, C.F. The impact of four dynamic, goal-steered treatment strategies on the 5-year outcomes of rheumatoid arthritis patients in the BeSt study. *Ann Rheum Dis*. 2011;70(6):1039-1046.
6. Siebert, S., Tsoukas, A., Robertson, J., and McInnes, I. Cytokines as therapeutic targets in rheumatoid arthritis and other inflammatory diseases. *Pharmacol Rev*. 2015;67(2):280-309.
7. Serhan, C.N. Pro-resolving lipid mediators are leads for resolution physiology. *Nature*. 2014;510(7503):92-101.
8. Chiang, N., Fredman, G., Backhed, F., Oh, S.F., Vickery, T., Schmidt, B.A., and Serhan, C.N. Infection regulates pro-resolving mediators that lower antibiotic requirements. *Nature*. 2012;484(7395):524-528.
9. Goldberg, R.J., and Katz, J. A meta-analysis of the analgesic effects of omega-3 polyunsaturated fatty acid supplementation for inflammatory joint pain. *Pain*. 2007;129(1-2):210-223.
10. Calder, P.C. Omega-3 polyunsaturated fatty acids and inflammatory processes: nutrition or pharmacology? *Br J Clin Pharmacol*. 2013;75(3):645-662.
11. Sun, Y.P., Oh, S.F., Uddin, J., Yang, R., Gotlinger, K., Campbell, E., Colgan, S.P., Petasis, N.A., and Serhan, C.N. Resolvin D1 and its aspirin-triggered 17R epimer. Stereochemical assignments, anti-inflammatory properties, and enzymatic inactivation. *J Biol Chem*. 2007;282(13):9323-9334.
12. Monach, P., Hattori, K., Huang, H., Hyatt, E., Morse, J., Nguyen, L., Ortiz-Lopez, A., Wu, H.J., Mathis, D., and Benoist, C. The K/BxN mouse model of inflammatory arthritis: theory and practice. *Methods Mol Med*. 2007;136269-282.
13. Colas, R.A., Shinohara, M., Dalli, J., Chiang, N., and Serhan, C.N. Identification and signature profiles for pro-resolving and inflammatory lipid mediators in human tissue. *Am J Physiol Cell Physiol*. 2014;307(1):C39-54.
14. Dalli, J., Winkler, J.W., Colas, R.A., Arnardottir, H., Cheng, C.Y., Chiang, N., Petasis, N.A., and Serhan, C.N. Resolvin D3 and aspirin-triggered resolvin D3 are potent immunoresolvents. *Chem Biol*. 2013;20(2):188-201.
15. Norling, L.V., Dalli, J., Flower, R.J., Serhan, C.N., and Perretti, M. Resolvin D1 limits polymorphonuclear leukocyte recruitment to inflammatory loci:

receptor-dependent actions. *Arterioscler Thromb Vasc Biol*. 2012;32(8):1970-1978.

16. Chou, R.C., Kim, N.D., Sadik, C.D., Seung, E., Lan, Y., Byrne, M.H., Haribabu, B., Iwakura, Y., and Luster, A.D. Lipid-cytokine-chemokine cascade drives neutrophil recruitment in a murine model of inflammatory arthritis. *Immunity*. 2010;33(2):266-278.
17. Schwab, J.M., Chiang, N., Arita, M., and Serhan, C.N. Resolvin E1 and protectin D1 activate inflammation-resolution programmes. *Nature*. 2007;447(7146):869-874.
18. Bannenberg, G.L., Chiang, N., Ariel, A., Arita, M., Tjonahen, E., Gotlinger, K.H., Hong, S., and Serhan, C.N. Molecular circuits of resolution: formation and actions of resolvins and protectins. *J Immunol*. 2005;174(7):4345-4355.
19. Chen, M., Lam, B.K., Kanaoka, Y., Nigrovic, P.A., Audoly, L.P., Austen, K.F., and Lee, D.M. Neutrophil-derived leukotriene B4 is required for inflammatory arthritis. *J Exp Med*. 2006;203(4):837-842.
20. Greco, K.V., Iqbal, A.J., Rattazzi, L., Nalesso, G., Moradi-Bidhendi, N., Moore, A.R., Goldring, M.B., Dell'Accio, F., and Perretti, M. High density micromass cultures of a human chondrocyte cell line: a reliable assay system to reveal the modulatory functions of pharmacological agents. *Biochem Pharmacol*. 2011;82(12):1919-1929.
21. Headland, S.E., Jones, H.R., Norling, L.V., Kim, A., Souza, P.R., Corsiero, E., Gil, C.D., Nerviani, A., Dell'Accio, F., Pitzalis, C., et al. Neutrophil-derived microvesicles enter cartilage and protect the joint in inflammatory arthritis. *Sci. Transl. Med.* 2015;7315ra190.
22. Dufton, N., Hannon, R., Brancaleone, V., Dalli, J., Patel, H.B., Gray, M., D'Acquisto, F., Buckingham, J.C., Perretti, M., and Flower, R.J. Anti-inflammatory role of the murine formyl-peptide receptor 2: ligand-specific effects on leukocyte responses and experimental inflammation. *J Immunol*. 2010;184(5):2611-2619.
23. Scher, J.U., Ubeda, C., Equinda, M., Khanin, R., Buischi, Y., Viale, A., Lipuma, L., Attur, M., Pillinger, M.H., Weissmann, G., et al. Periodontal disease and the oral microbiota in new-onset rheumatoid arthritis. *Arthritis Rheum*. 2012;64(10):3083-3094.
24. Perretti, M., Leroy, X., Bland, E.J., and Montero-Melendez, T. Resolution Pharmacology: Opportunities for Therapeutic Innovation in Inflammation. *Trends Pharmacol Sci*. 2015;36(11):737-755.
25. Caliendo, G., Cirino, G., Santagada, V., and Wallace, J.L. Synthesis and biological effects of hydrogen sulfide (H2S): development of H2S-releasing drugs as pharmaceuticals. *J Med Chem*. 2010;53(17):6275-6286.
26. Dalli, J., Kraft, B.D., Colas, R.A., Shinohara, M., Fredenburgh, L.E., Hess, D.R., Chiang, N., Welty-Wolf, K.E., Choi, A.M., Piantadosi, C.A., et al. Proresolving Lipid Mediator Profiles in Baboon Pneumonia are Regulated by Inhaled Carbon Monoxide. *Am J Respir Cell Mol Biol*. 2015.
27. Chiang, N., Shinohara, M., Dalli, J., Mirakaj, V., Kibi, M., Choi, A.M., and Serhan, C.N. Inhaled carbon monoxide accelerates resolution of inflammation via unique proresolving mediator-heme oxygenase-1 circuits. *J Immunol*. 2013;190(12):6378-6388.

28. Yacoubian, S., and Serhan, C.N. New endogenous anti-inflammatory and proresolving lipid mediators: implications for rheumatic diseases. *Nat Clin Pract Rheumatol*. 2007;3(10):570-579; quiz 571 p following 589.
29. Kronke, G., Katzenbeisser, J., Uderhardt, S., Zaiss, M.M., Scholtysek, C., Schabbauer, G., Zarbock, A., Koenders, M.I., Axmann, R., Zwerina, J., et al. 12/15-lipoxygenase counteracts inflammation and tissue damage in arthritis. *J Immunol*. 2009;183(5):3383-3389.
30. Dufton, N., Hannon, R., Brancaleone, V., Dalli, J., Patel, H.B., Gray, M., D'Acquisto, F., Buckingham, J.C., Perretti, M., and Flower, R.J. Anti-inflammatory role of the murine formyl-peptide receptor 2: ligand-specific effects on leukocyte responses and experimental inflammation. *Journal of immunology*. 2010;184(5):2611-2619.
31. Blaho, V.A., Zhang, Y., Hughes-Hanks, J.M., and Brown, C.R. 5-Lipoxygenase-deficient mice infected with Borrelia burgdorferi develop persistent arthritis. *Journal of immunology*. 2011;186(5):3076-3084.
32. Chan, M.M., and Moore, A.R. Resolution of inflammation in murine autoimmune arthritis is disrupted by cyclooxygenase-2 inhibition and restored by prostaglandin E2-mediated lipoxin A4 production. *J Immunol*. 2010;184(11):6418-6426.
33. Leslie, C.A., Gonnerman, W.A., Ullman, M.D., Hayes, K.C., Franzblau, C., and Cathcart, E.S. Dietary fish oil modulates macrophage fatty acids and decreases arthritis susceptibility in mice. *J Exp Med*. 1985;162(4):1336-1349.
34. Leslie, C.A., Conte, J.M., Hayes, K.C., and Cathcart, E.S. A fish oil diet reduces the severity of collagen induced arthritis after onset of the disease. *Clin Exp Immunol*. 1988;73(2):328-332.
35. Gheorghe, K.R., Korotkova, M., Catrina, A.I., Backman, L., af Klint, E., Claesson, H.E., Radmark, O., and Jakobsson, P.J. Expression of 5-lipoxygenase and 15-lipoxygenase in rheumatoid arthritis synovium and effects of intraarticular glucocorticoids. *Arthritis Res Ther*. 2009;11(3):R83.
36. Hashimoto, A., Hayashi, I., Murakami, Y., Sato, Y., Kitasato, H., Matsushita, R., Iizuka, N., Urabe, K., Itoman, M., Hirohata, S., et al. Antiinflammatory mediator lipoxin A4 and its receptor in synovitis of patients with rheumatoid arthritis. *J Rheumatol*. 2007;34(11):2144-2153.
37. Giera, M., Ioan-Facsinay, A., Toes, R., Gao, F., Dalli, J., Deelder, A.M., Serhan, C.N., and Mayboroda, O.A. Lipid and lipid mediator profiling of human synovial fluid in rheumatoid arthritis patients by means of LC-MS/MS. *Biochimica et biophysica acta*. 2012;1821(11):1415-1424.
38. Wright, H.L., Moots, R.J., and Edwards, S.W. The multifactorial role of neutrophils in rheumatoid arthritis. *Nat Rev Rheumatol*. 2014;10(10):593-601.
39. Norling, L.V., Dalli, J., Flower, R.J., Serhan, C.N., and Perretti, M. Resolvin D1 limits polymorphonuclear leukocyte recruitment to inflammatory loci: receptor-dependent actions. *Arteriosclerosis, thrombosis, and vascular biology*. 2012;32(8):1970-1978.
40. Norling, L.V., Spite, M., Yang, R., Flower, R.J., Perretti, M., and Serhan, C.N. Cutting edge: Humanized nano-proresolving medicines mimic inflammation-resolution and enhance wound healing. *J Immunol*. 2011;186(10):5543-5547.
41. Krishnamoorthy, S., Recchiuti, A., Chiang, N., Fredman, G., and Serhan, C.N. Resolvin D1 receptor stereoselectivity and regulation of inflammation and

proresolving microRNAs. *The American journal of pathology*. 2012;180(5):2018-2027.

42. Tang, Y., Zhang, M.J., Hellmann, J., Kosuri, M., Bhatnagar, A., and Spite, M. Proresolution therapy for the treatment of delayed healing of diabetic wounds. *Diabetes*. 2013;62(2):618-627.
43. Hasturk, H., Kantarci, A., Goguet-Surmenian, E., Blackwood, A., Andry, C., Serhan, C.N., and Van Dyke, T.E. Resolvin E1 regulates inflammation at the cellular and tissue level and restores tissue homeostasis in vivo. *J Immunol*. 2007;179(10):7021-7029.
44. Dalli, J., Zhu, M., Vlasenko, N.A., Deng, B., Haeggstrom, J.Z., Petasis, N.A., and Serhan, C.N. The novel 13S,14S-epoxy-maresin is converted by human macrophages to maresin 1 (MaR1), inhibits leukotriene A4 hydrolase (LTA4H), and shifts macrophage phenotype. *FASEB J*. 2013;27(7):2573-2583.
45. Leoni, G., Neumann, P.A., Kamaly, N., Quiros, M., Nishio, H., Jones, H.R., Sumagin, R., Hilgarth, R.S., Alam, A., Fredman, G., et al. Annexin A1-containing extracellular vesicles and polymeric nanoparticles promote epithelial wound repair. *J Clin Invest*. 2015;125(3):1215-1227.
46. Spite, M., Norling, L.V., Summers, L., Yang, R., Cooper, D., Petasis, N.A., Flower, R.J., Perretti, M., and Serhan, C.N. Resolvin D2 is a potent regulator of leukocytes and controls microbial sepsis. *Nature*. 2009;461(7268):1287-1291.
47. Chiang, N., Dalli, J., Colas, R.A., and Serhan, C.N. Identification of resolvin D2 receptor mediating resolution of infections and organ protection. *J Exp Med*. 2015;212(8):1203-1217.
48. Hasturk, H., Kantarci, A., Ohira, T., Arita, M., Ebrahimi, N., Chiang, N., Petasis, N.A., Levy, B.D., Serhan, C.N., and Van Dyke, T.E. RvE1 protects from local inflammation and osteoclast- mediated bone destruction in periodontitis. *FASEB J*. 2006;20(2):401-403.
49. Herrera, B.S., Ohira, T., Gao, L., Omori, K., Yang, R., Zhu, M., Muscara, M.N., Serhan, C.N., Van Dyke, T.E., and Gyurko, R. An endogenous regulator of inflammation, resolvin E1, modulates osteoclast differentiation and bone resorption. *Br J Pharmacol*. 2008;155(8):1214-1223.
50. McCauley, L.K., Dalli, J., Koh, A.J., Chiang, N., and Serhan, C.N. Cutting edge: Parathyroid hormone facilitates macrophage efferocytosis in bone marrow via proresolving mediators resolvin D1 and resolvin D2. *J Immunol*. 2014;193(1):26-29.
51. Ji, R.R., Xu, Z.Z., Strichartz, G., and Serhan, C.N. Emerging roles of resolvins in the resolution of inflammation and pain. *Trends Neurosci*. 2011;34(11):599-609.
52. Lima-Garcia, J.F., Dutra, R.C., da Silva, K., Motta, E.M., Campos, M.M., and Calixto, J.B. The precursor of resolvin D series and aspirin-triggered resolvin D1 display anti-hyperalgesic properties in adjuvant-induced arthritis in rats. *Br J Pharmacol*. 2011;164(2):278-293.
53. Kasuga, K., Yang, R., Porter, T.F., Agrawal, N., Petasis, N.A., Irimia, D., Toner, M., and Serhan, C.N. Rapid appearance of resolvin precursors in inflammatory exudates: novel mechanisms in resolution. *J Immunol*. 2008;181(12):8677-8687.

54. Goldring, M.B., Birkhead, J.R., Suen, L.F., Yamin, R., Mizuno, S., Glowacki, J., Arbiser, J.L., and Apperley, J.F. Interleukin-1 beta-modulated gene expression in immortalized human chondrocytes. *J Clin Invest*. 1994;94(6):2307-2316.

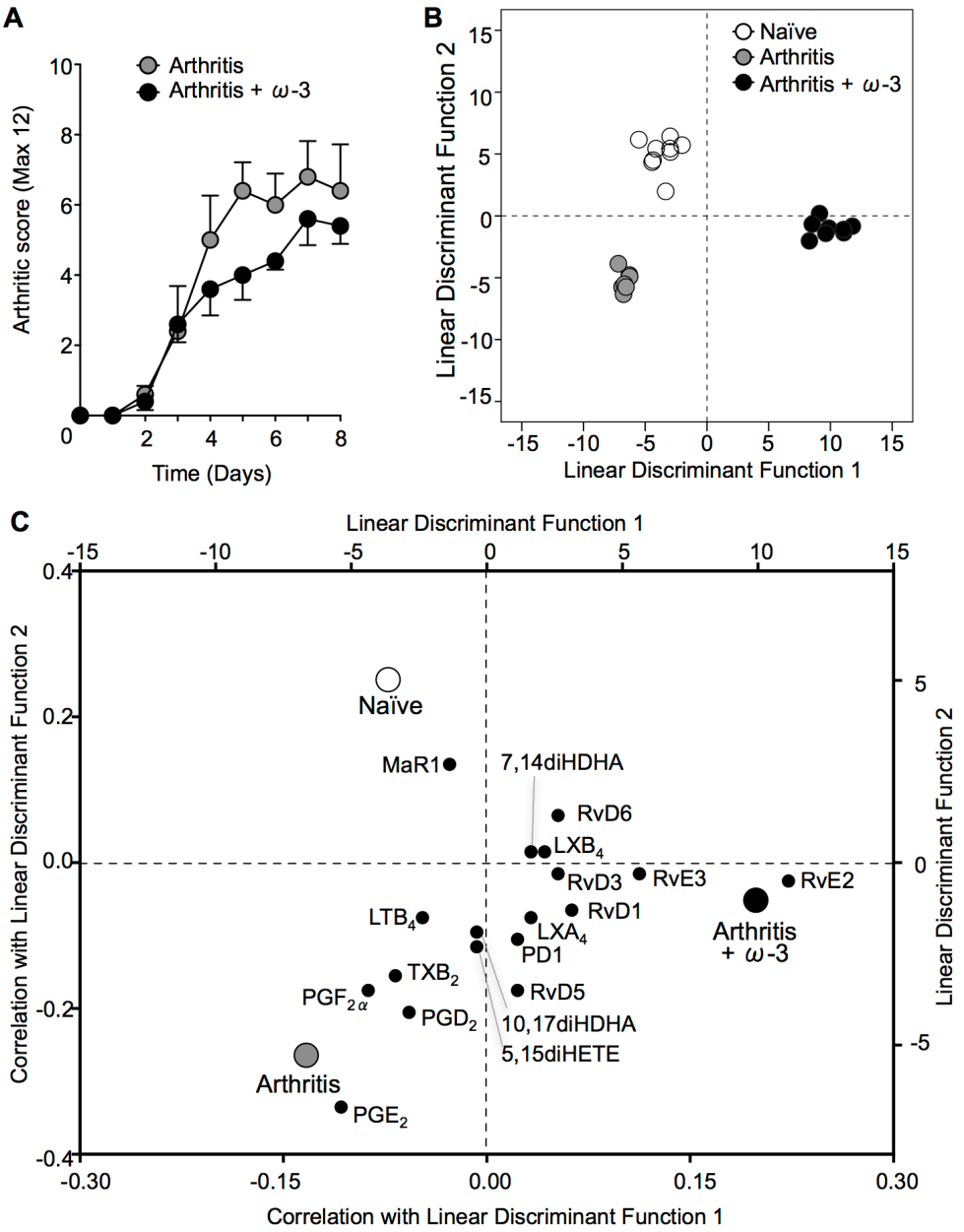


**Figure 1. Mice fed an omega-3 supplemented diet display reduced arthritis and a modulated local biosynthesis of bioactive lipids within arthritic joints.** Mice fed a standard or omega-3 supplemented diet were given arthritogenic serum (100µl, i.p. on days 0 and 2) and **(A)** arthritic score was evaluated **(B)** Arthritic paws were collected for metabololipidomics analysis on day 8. Linear discriminant analysis was used to generate two discriminant functions from the values of bioactive lipid mediators (as quantified by LC-MS/MS), which maximize the difference between naïve, arthritis and arthritis + omega-3 treatment groups. Each datum corresponds to an individual mouse. The model achieves complete discrimination of the three groups. (**C**) Correlations of each lipid mediator with the two linear discriminant functions are shown on the bottom x and left y axes. Group centroids for the two discriminant functions are plotted on the top x and right y axes to show the directionality and association of each lipid with the three treatment groups. *n*=7-9 mice per group.

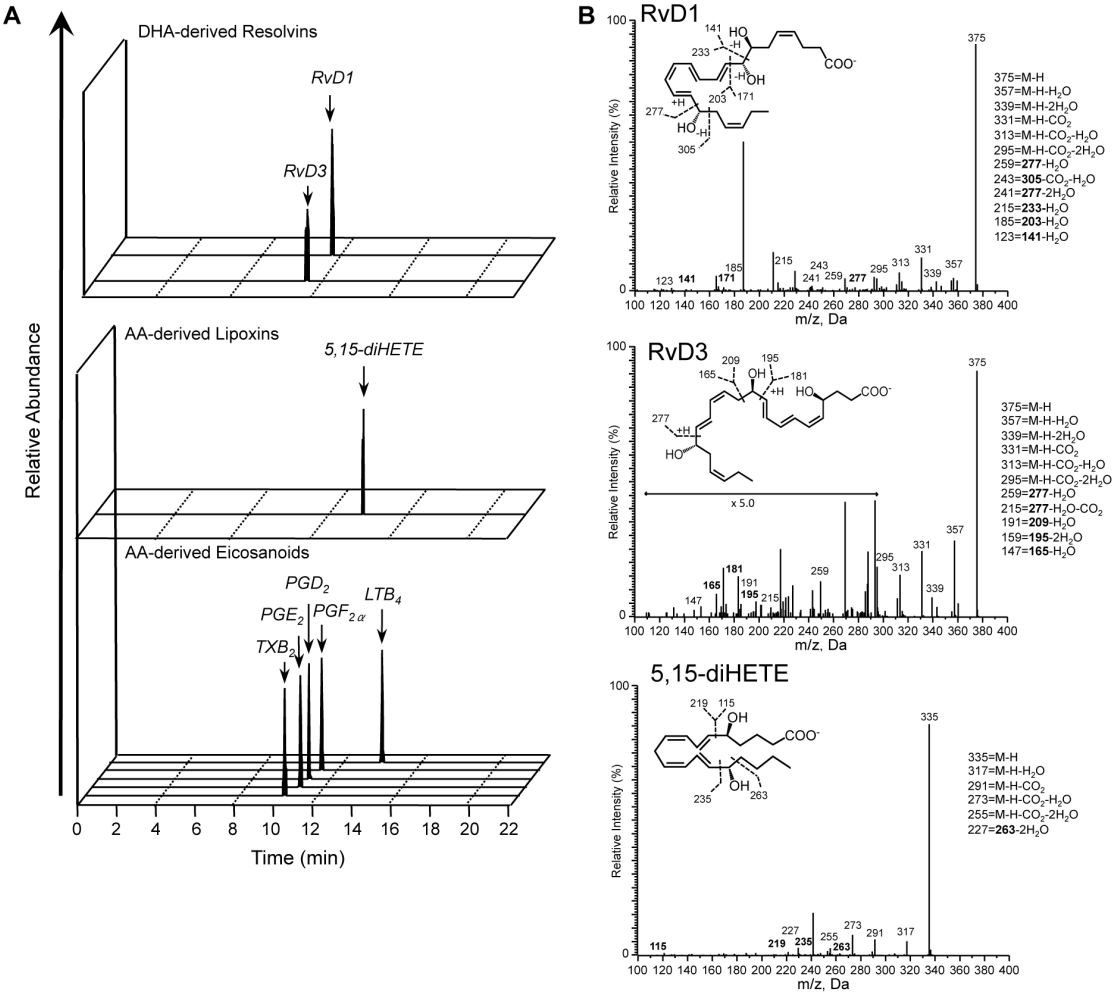


**Figure 2. Identification of Resolvin D1 and D3 in synovial fluids from Rheumatoid arthritis (RA) patients.** Lipid mediator levels were assessed following solid phase extraction by liquid chromatography tandem mass spectrometry (LC-MS/MS) based metabololipidomics (see methods for details). **(A)** Representative multiple reaction monitoring (MRM) traces for the identified lipid mediators in human RA synovial fluids (from *n*=4). **(B)** Accompanying MS/MS spectra utilised for identification. Refer to Table 2 for patient demographics and Table 3 for quantification of bioactive lipid mediators.

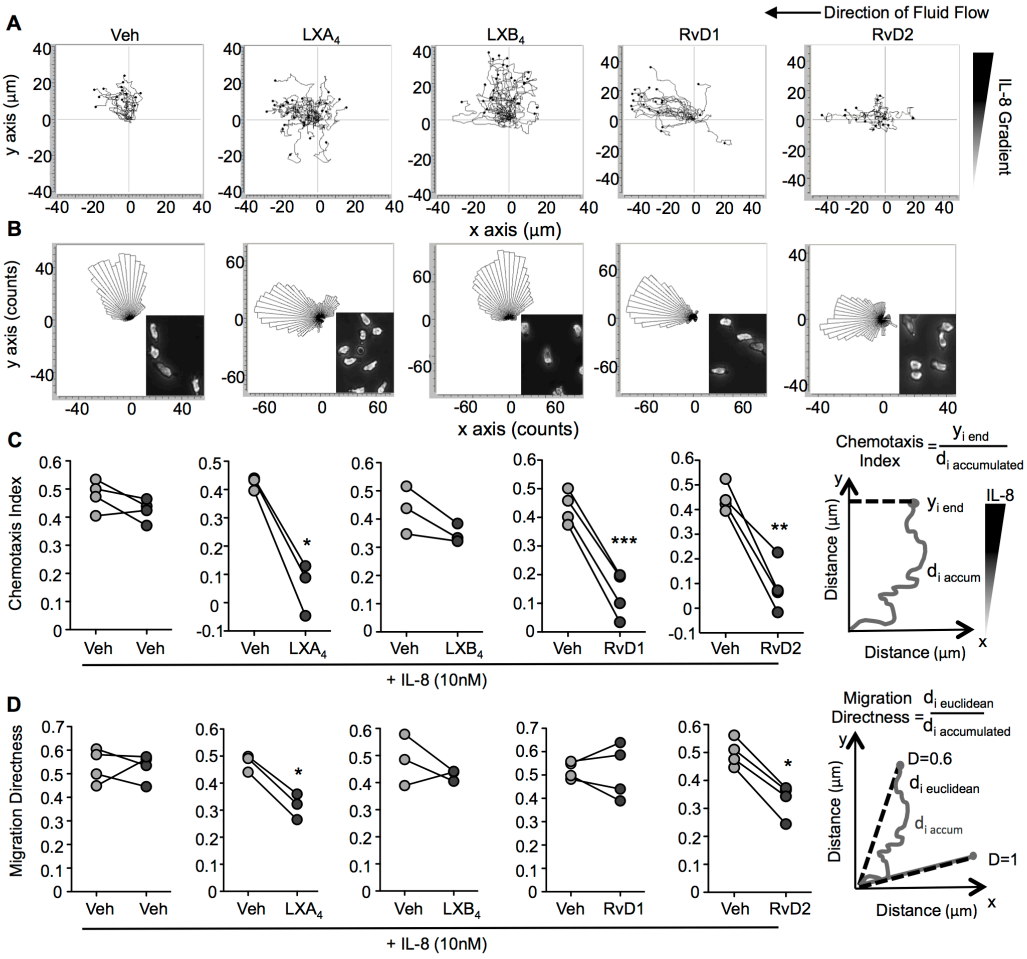


**Figure 3. Direct actions of RvD1, RvD2, $LXA_4$ and $LXB_4$ on human neutrophil chemotaxis.** Neutrophils were captured from whole blood of healthy volunteers on P-selectin and ICAM-1-coated microfluidics chambers. Chemotaxis towards an IL-8 gradient (10nM) was monitored in real-time over 30 min. During the first 15 min cells were exposed to HBSS + IL-8 (0-10nM vertical gradient), then cells were exposed to a set concentration of resolvin D1 (RvD1), RvD2, lipoxin $A_4$ ($LXA_4$) or $LXB_4$ (1nM) or vehicle (HBSS + 0.1% ethanol) together with the IL-8 gradient over the subsequent 15 min. **(A)** Representative trajectory paths and **(B)** rose plots of migrating cells are shown. Insets in B show morphology of neutrophils after exposure to IL-8 or pro-resolving mediators. **(C)** Quantification of neutrophil chemotaxis index **(D)** and directness of neutrophil migration as depicted by the graphs, *n*=3-4 donors per compound. **P*<0.05 ***P*<0.01 and ****P*<0.001 with two-tailed paired Student's t-tests.

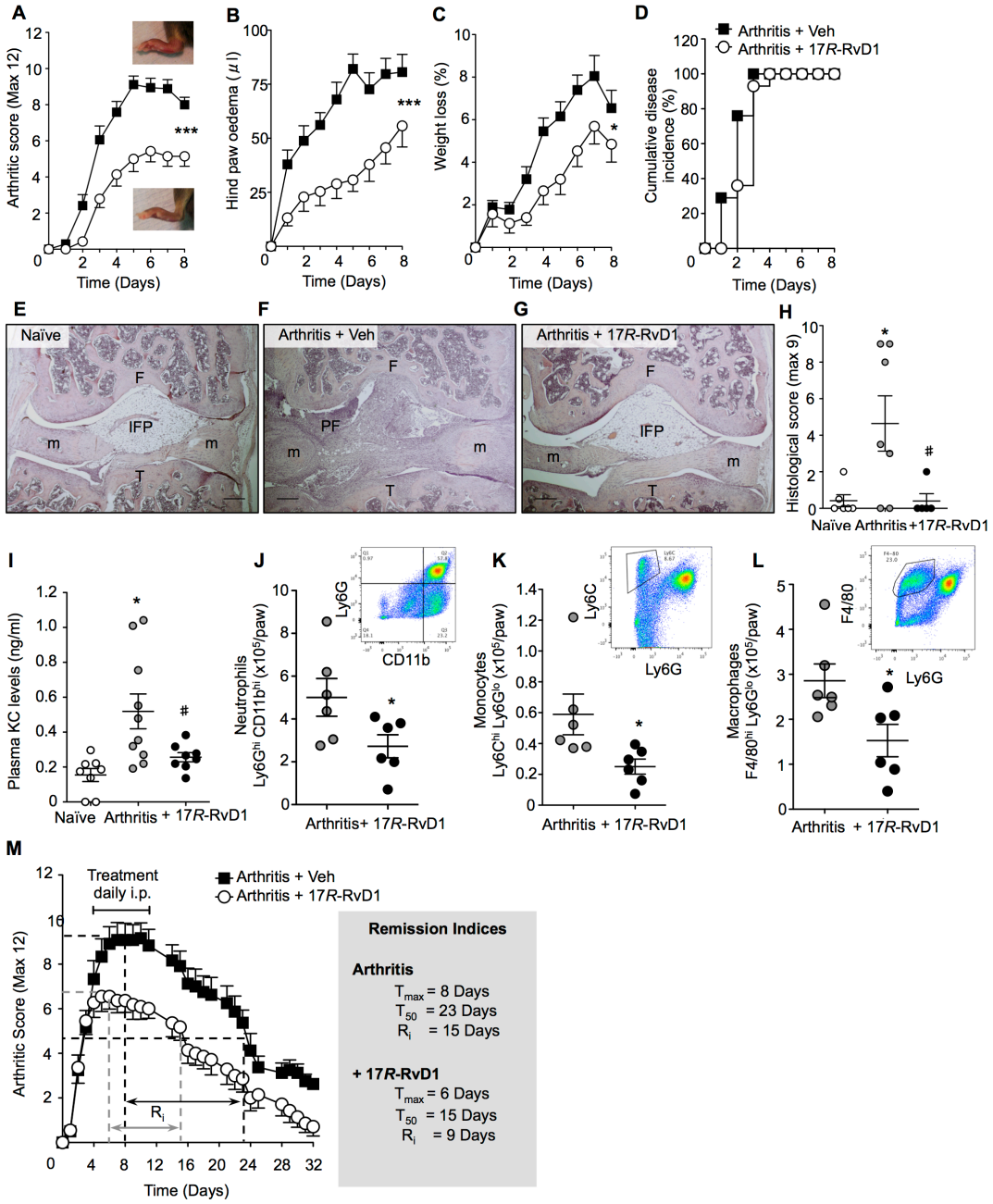


**Figure 4. 17*R*-RvD1 suppresses inflammatory arthritis by limiting leukocyte infiltration to arthritic joints.** Arthritis was induced with arthritogenic serum (100μl, i.p. on days 0 and 2). Mice were treated daily with vehicle (0.1% ethanol) or 17*R*-RvD1 (100ng) and **(A)** arthritic score, **(B)** paw edema **(C)** weight loss and **(D)** disease incidence were evaluated. *Inset* in A are representative photographs of hind paw arthritis with and without daily 17*R*-RvD1 treatment, *n*=14-17 mice per group. ***$P$<0.001 or *$P$<0.05 two-way ANOVA with repeated measures. **(E-G)** Representative hematoxylin and eosin stained sections of knees from naïve and arthritic mice on day 8 after arthritis induction (x4 magnification), from *n*=5-7 mice per group. Scale bars 200μm, F, femur; T, tibia; m, meniscus; IFP, infrapatellar fat pad; PF, pannus formation. **(H)** Histological score calculated by degree of leukocyte

infiltration, cartilage and bone erosion, $n$=5-7 mice per group, *$P$<0.05 vs. naïve, $^{\#}P$<0.05 vs. arthritis, one-way ANOVA with Bonferroni post-hoc test **(I)** Plasma KC levels, $n$=8-10 mice per group, *$P$<0.05 one-way ANOVA with Bonferroni post-hoc test **(J-L)** Arthritic paws were digested to liberate leukocytes; cells were counted by light microscopy and leukocyte subsets defined using specific antibodies by flow cytometry, $n$=6 mice per group, *$P$<0.05 unpaired Student's t-test **(M)** Mice were treated daily following overt signs of arthritis (day 4) for one week with vehicle (0.1% ethanol) or 17$R$-RvD1 (100ng) and arthritic score was evaluated over 32 days and arthritis remission indices were calculated $n$=11-12 mice per group.

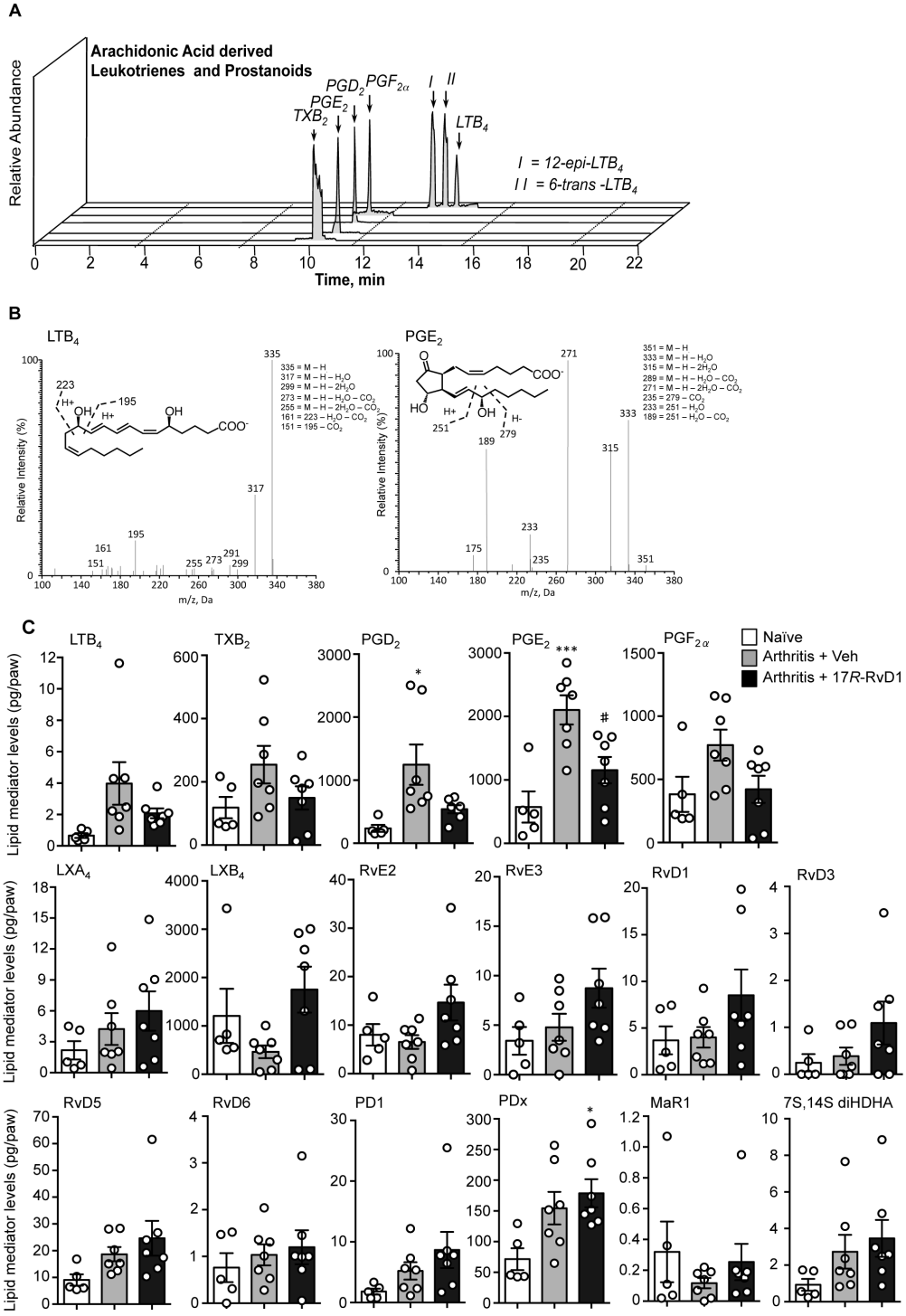


**Figure 5. 17*R*-RvD1 treatments modulate the local production of bioactive lipid mediators within inflamed paws.** Arthritic mice were treated daily with vehicle (0.1% ethanol) or 17*R*-RvD1 (100ng) and paws were collected for metabololipidomics analysis on day 8, naïve mice were used as controls. **(A)** Relative abundance of key arachidonic acid derived leukotrienes and prostanoids. Representative mass spectrum of **(B)** $LTB_4$ and **(C)** $PGE_2$ within arthritic paws. **(D-T)** Absolute quantification of lipid mediator levels in arthritic paws identified using scheduled multiple reaction monitoring (MRM). *n*=5-7 per group. **P*<0.05 and

***$P$<0.001 vs. naïve and $^{\#}P$<0.05 vs. arthritis with one-way ANOVA and Bonferroni post-hoc test.

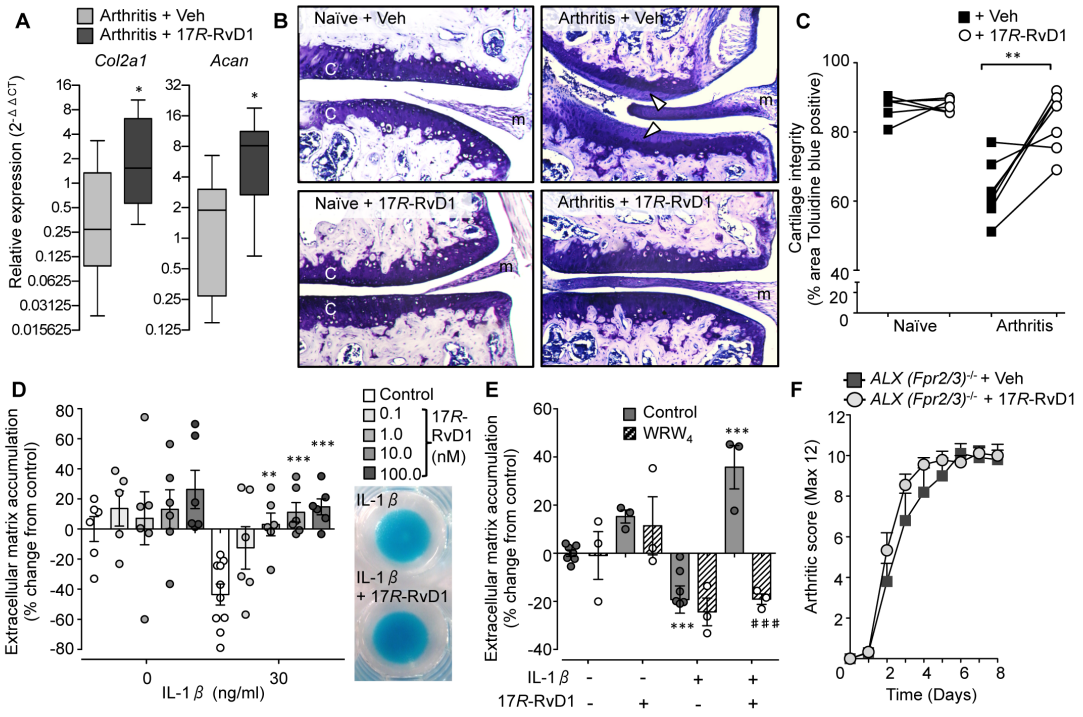


**Figure 6. Intra-articular treatment with 17*R*-RvD1 protects from cartilage degradation during inflammatory arthritis. (A)** Arthritis was induced with arthritogenic serum (100µl, days 0 and 2), mice were treated daily with vehicle (0.1% EtOH) or 17*R*-RvD1 (100ng, i.p.) and paws were collected for gene expression analysis on day 8 (see methods), *n*=8-9 mice per group **P*<0.05 with Mann-Whitney t-test. **(B-C)** Mice received arthritogenic serum (100µl, i.p. days 0 and 2), and were treated locally on day 3 with vehicle (left knee, 5µl PBS containing 0.1% EtOH) or 17*R*-RvD1 (right knee; 5µl, 100ng 17*R*-RvD1). On day 5, knee joints were collected and stained with toluidine blue, *n*=7 mice per group. Naïve mice were administered vehicle or 17*R*-RvD1 locally and knees collected after 2 days, *n*=6 mice per group. **(B)** Representative images (x20 magnification) of histological sections from naïve and arthritic joints are shown. C, cartilage; m, meniscus. Loss of glycosaminoglycans indicated by Δ **(C)** Cartilage integrity calculated from percentage area of cartilage positive for toluidine blue staining, ***P*<0.01 with two-tailed paired Student's t-test **(D-E)** In vitro analyses of chondroprotection utilising human C28/I2 micromasses. **(D)** Micromasses were treated with or without IL-1β (30ng/ml) alone or with 17*R*-RvD1 (0.1-100nM) and ECM accumulation evaluated (see methods), *n*=6-10 per group, ***P*<0.01, ****P*<0.001 vs. IL-1β with two-way ANOVA and Bonferroni post-test. *Inset* representative micromasses stained with Alcian blue prior to dye extraction. **(E)** FPR2/ALX receptor antagonist $WRW_4$ (10µM) was added to micromasses 10min prior to 17*R*-RvD1 and ECM accumulation evaluated after 24h, *n*=3-7 per group, ****P*<0.001 vs. vehicle, $^{\#\#\#}P$<0.001 vs. respective control with two-way ANOVA and Bonferroni post-test. **(F)** Dependency of *Fpr2/3* (ALX) receptor for 17*R*-RvD1 protection from inflammatory arthritis. Arthritis was induced in *Fpr2/3* (ALX) null mice (see methods), mice were treated daily with vehicle (PBS with 0.1% EtOH) or 17*R*-RvD1 (100ng, i.p.) and arthritic score assessed, *n*=9-10 mice per group.

| Bioactive LM/ Pathway Precursors | | | Lipid mediator levels (pg/paw) | | |
|---|---|---|---|---|---|
| | *Q1* | *Q3* | Naïve | Arthritis | Arthritis + Omega-3 |
| **DHA Metabolome** | | | | | |
| RvD1 | *375* | *215* | 2.3 ± 1.0 | 4.0 ± 1.1 | 6.6 ± 1.4* |
| RvD2 | *375* | *215* | - | - | - |
| RvD3 | *375* | *181* | 0.3 ± 0.2 | 0.4 ± 0.2 | 1.5 ± 0.9 |
| RvD5 | *359* | *199* | 9.6 ± 1.3 | 18.7 ± 2.7** | 16.6 ± 1.6* |
| RvD6 | *359* | *101* | 2.4 ± 0.7 | 1.0 ± 0.2 | 3.1 ± 0.7 |
| PD1 | *359* | *153* | 2.5 ± 0.5 | 5.2 ± 1.4 | 5.0 ± 1.0 |
| 10*S*,17*S*-diHDHA | *359* | *153* | 93.6 ± 16.8 | 154.5 ± 26.5 | 123.3 ± 17.7 |
| MaR1 | *359* | *221* | 3.1 ± 1.3 | 0.1 ± 0.0* | 0.3 ± 0.1 |
| 7*S*,14*S*-diHDHA | *359* | *221* | 3.3 ± 1.1 | 2.7 ± 0.9 | 4.2 ± 0.6 |
| 17-HDHA | *343* | *245* | 313.5 ± 65.9 | 591.1 ± 133.3 | 1030.9 ± 200.4** |
| 14-HDHA | *343* | *205* | 859.7 ± 227.3 | 1910.4 ± 331.5 | 2930.1 ± 550.1** |
| 7-HDHA | *343* | *141* | 52.9 ± 8.6 | 49.2 ± 5.3 | 156.9 ± 11.1$^{\#\#}$* |
| 4-HDHA | *343* | *101* | 109.8 ± 19.2 | 70.6 ± 4.4 | 260.6 ± 25.7$^{\#\#}$* |
| **AA Metabolome** | | | | | |
| $LXA_4$ | *351* | *115* | 1.3 ± 0.6 | 4.2 ± 1.5 | 5.1 ± 2.1 |
| $LXB_4$ | *351* | *221* | 122.6 ± 65.8 | 84.2 ± 23.7 | 199.9 ± 47.9 |
| 5*S*,15*S*-diHETE | *351* | *221* | 3.4 ± 0.4 | 7.2 ± 1.9 | 5.0 ± 0.9 |
| $LTB_4$ | *335* | *195* | 1.8 ± 0.6 | 4.0 ± 1.4 | 1.5 ± 0.2 |
| $PGE_2$ | *351* | *189* | 353.0 ± 156.8 | 2103.4 ± 229.0*** | 628.0 ± 89.8$^{\#\#\#}$ |
| $PGD_2$ | *351* | *189* | 155.1 ± 44.5 | 1246.3 ± 320.1*** | 398.4 ± 68.9$^{\#\#}$ |
| $PGF_{2\alpha}$ | *353* | *193* | 219.5 ± 97.5 | 770.9 ± 123.2** | 194.8 ± 36.8$^{\#\#\#}$ |
| $TxB_2$ | *369* | *169* | 73.0 ± 25.4 | 254.4 ± 59.2** | 73.6 ± 14.3$^{\#\#}$ |
| 5-HETE | *319* | *219* | 632.1 ± 129.6 | 1617.5 ± 508.2 | 804.2 ± 228.5 |
| 12-HETE | *319* | *179* | 1453.4 ± 381.4 | 3849.1 ± 1041.0 | 1923.7 ± 543.3 |
| 15-HETE | *319* | *115* | 165.8 ± 22.7 | 271.2 ± 19.4** | 176.9 ± 16.6$^{\#}$ |
| **EPA Metabolome** | | | | | |
| RvE1 | *349* | *195* | - | - | - |
| RvE2 | *333* | *253* | 9.7 ± 1.7 | 6.5 ± 1.4 | 39.2 ± 5.2$^{\#\#}$* |
| RvE3 | *333* | *201* | 7.1 ± 1.8 | 4.8 ± 1.4 | 51.5 ± 16.7$^{\#}$* |
| 18-HEPE | *317* | *259* | 100.2 ± 21.9 | 42.5 ± 3.8 | 1213.6 ± 183.2$^{\#\#\#}$*** |
| 15-HEPE | *317* | *219* | 493.5 ± 97.9 | 1589.4 ± 578.3 | 4470.9 ± 815.5$^{\#\#}$*** |
| 12-HEPE | *317* | *179* | 228.8 ± 32.9 | 377.2 ± 139.0 | 1583.3 ± 298.1$^{\#\#\#}$*** |
| 5-HEPE | *317* | *115* | 48.5 ± 6.5 | 40.2 ± 3.1 | 707.6 ± 78.8$^{\#\#\#}$* |

**Table 1. Bioactive SPM and pathway precursors identified in murine naïve and arthritic joints.** Naïve or arthritic mouse paws were collected for metabololipidomics analysis on day 8 (see methods for details). Quantification of bioactive lipid mediators (LM) and pathway precursors were assessed by liquid chromatography tandem mass spectrometry (LC-MS/MS) based metabololipidomics. Results are expressed as pg/paw. Q1: M-H (parent ion) and Q3 (daughter ion): diagnostic ion in the MS-MS. Detection limit was ~ 0.1 pg; - denotes below limits. Results are mean ± SEM from 7-9 mice per group. *$P$<0.05 **$P$<0.01 and ***$P$<0.001 compared to naïve and $^{\#}P$<0.05, $^{\#\#}P$<0.01 *and* $^{\#\#\#}P$<0.001 compared to arthritic with one-way ANOVA and Tukey's multiple comparison test.

| Diagnosis/ Sample type | Age/ Gender | Ethnicity | ACR Functional Class/Disease Activity | CRP (mg/ L) | RA Medication |
|---|---|---|---|---|---|
| Rheumatoid arthritis/ Synovial fluid | 70/M | Caucasian | Moderate | 20 | Enbrel Sure Stick 50mg/mL 50mg once a week, Celebrex 200mg 2 times/day, Acetaminophen 650mg 3 times/day |
| Rheumatoid arthritis/ Synovial fluid | 48/F | Caucasian | Functional Class III | 29.6 | Butran 5ug/h 1 patch/wk Rituxan 10mg/ml, 1000mg, Methotrexate 2.5mg 10 tabs/wk, Vit D3 1000IU 5 tabs, Prednisone 7mg/day, Folic acid 1 mg/day, Pennsaid 1.5% liquid 40 drops to painful area 4 times/day as needed, Roxicodone 5mg 1-2 tabs 2-3 times/day |
| Rheumatoid arthritis/ Synovial fluid | 40/F | Caucasian | Functional Class II | 17.2 | Humira 40mg SC QWK Meloxicam 15mg/day |
| Rheumatoid arthritis/ Synovial fluid | 74/F | Hispanic | Moderate | <3 | Leflunomide 10mg/day, Aleve 220mg as needed, Aspirin 81mg 2 times/day, Osteobiflex 1 tab/day |

**Table 2. Human rheumatoid arthritis patient demographics, disease status and medications at the time of sample collection.**

| | *Q1* | *Q3* | Synovial fluid (pg/mL) |
|---|---|---|---|
| **DHA Bioactive Metabolome** | | | |
| RvD1 | *375* | *215* | 11.7 ± 2.6 |
| RvD2 | *375* | *215* | - |
| RvD3 | *375* | *215* | 8.7 ± 3.3 |
| RvD5 | *359* | *199* | - |
| RvD6 | 359 | *101* | - |
| PD1 | *359* | *153* | - |
| MaR1 | *359* | *250* | - |
| **AA Bioactive Metabolome** | | | |
| $LXA_4$ | *351* | *115* | - |
| $LXB_4$ | *351* | *221* | - |
| 5,15-diHETE | *335* | *235* | 4.3 ± 1.7 |
| $LTB_4$ | *335* | *195* | 9.1 ± 3.9 |
| $PGE_2$ | *351* | *175* | 53.1 ± 23.8 |
| $PGD_2$ | *351* | *189* | 4.5 ± 1.3 |
| $PGF_{2\alpha}$ | *353* | *193* | 18.9 ± 5.2 |
| $TxB_2$ | *369* | *169* | 14.1 ± 4.1 |
| **EPA Bioactive Metabolome** | | | |
| RvE1 | *349* | *195* | - |
| RvE2 | *333* | *253* | - |
| 5,15-diHEPE | *333* | *235* | 2.1 ± 0.7 |

**Table 3. Lipid Mediator-SPM identified in human Rheumatoid arthritis (RA) synovial fluid.** Quantification of bioactive lipid mediators (LM) in human synovial fluid from RA patients assessed by liquid chromatography tandem mass spectrometry (LC-MS/MS) based lipid mediator (LM) metabololipidomics. Results are expressed as pg/mL synovial fluid. Q1: M-H (parent ion) and Q3 (daughter ion): diagnostic ion in the MS-MS. Detection limit was ~ 0.1 pg; - denotes below limits. Results are mean ± SEM. from 4 donors.

**Supplemental Data**

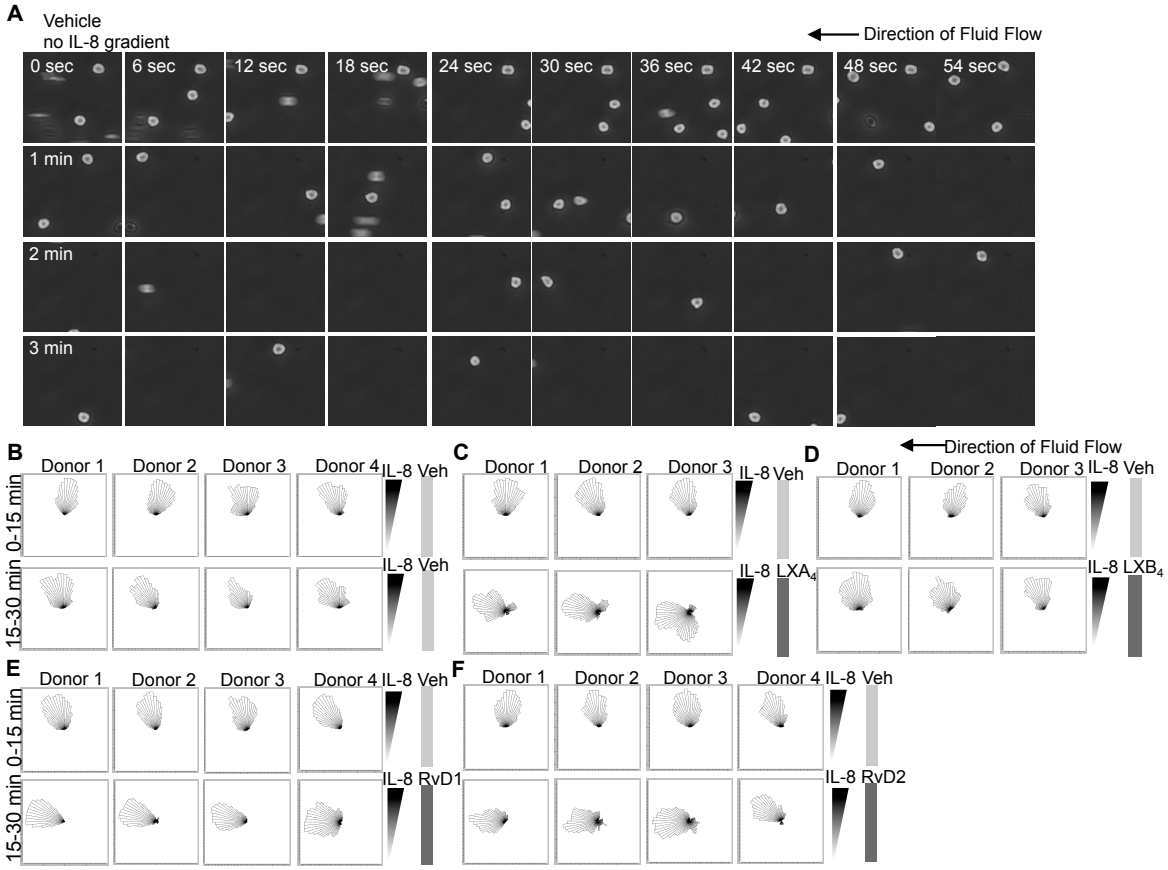


**Supplemental Figure 1. Neutrophil migration trajectories following exposure to Specialised pro-resolving lipid mediators (SPM).** Neutrophils were captured from whole blood of healthy volunteers on P-selectin and ICAM-1-coated microfluidics chambers. (A) Neutrophils remained rounded and rapidly detached in the absence of a chemotactic gradient. Cells were exposed to media plus vehicle (0.1% ethanol) and videos were captured in real-time over 15 min. Representative still images are shown for the first 4 min, taken every 6 sec. (B) Rose plots indicating migration trajectories from individual donors after exposure to an IL-8 gradient (10nM, 15min) followed by exposure to a set concentration of resolvin D1 (RvD1), RvD2, lipoxin $A_4$ ($LXA_4$) or $LXB_4$ (1nM, 15min) or vehicle together with the IL-8 gradient.

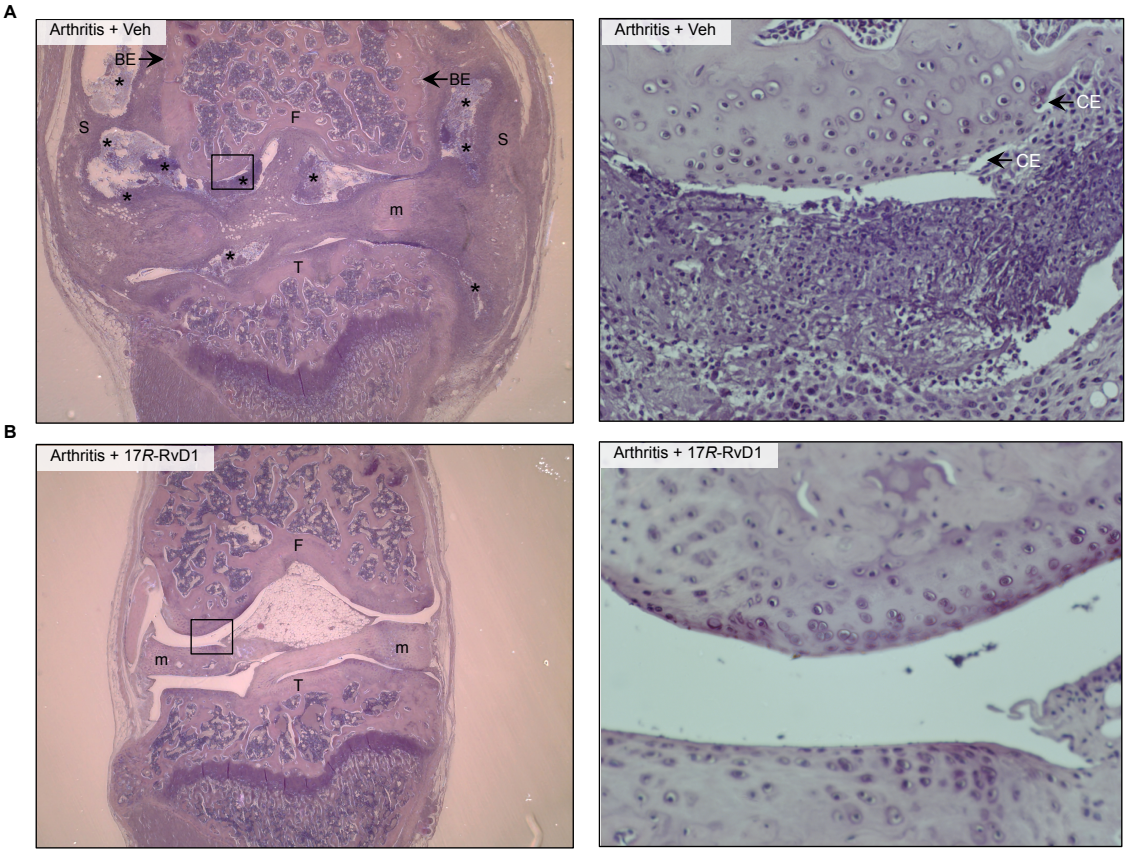


**Supplemental Figure 2. Histopathology of murine knee joints is improved with 17*R*-RvD1 treatment.** (A) Representative haematoxylin & eosin histology sections of knee joints from arthritic mice 8 days after arthritis induction following daily administration of vehicle (0.1% ethanol in PBS, i.p.) or (B) 17*R*-RvD1 (100ng, i.p.). Representative low (x4) and high (x20) power magnifications are shown for each genotype. F; femur, T; tibia, m; meniscus, PF; pannus formation, BE; bone erosion, S; synovitis, *; neutrophil infiltration, from *n*=5-7 mice per group.

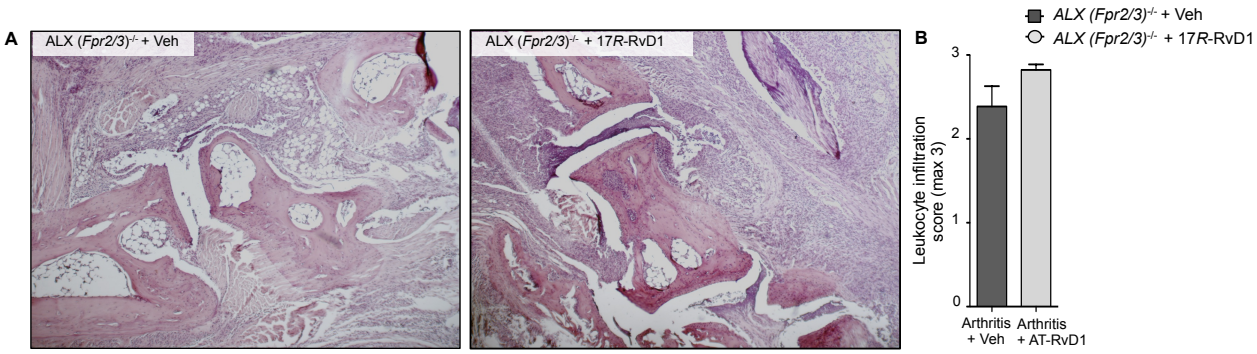


**Supplemental Figure 3. Joint protection from 17*R*-RvD1 is lost in *Fpr2/3* (ALX) null mice.** (A) Representative haematoxylin & eosin histology sections of murine arthritic hind paws 8 days after arthritis induction (x10 magnification). (B) Histological score calculated by degree of leukocyte infiltration (max. 3), *n*=5-6 mice per group.

| | Relative Expression (AU) | | |
|---|---|---|---|
| **Gene** | **Arthritis** | **Arthritis + 17*R*-RvD1** | **% Change** |
| ***Alox15*** | 1.76 ± 0.73 | 3.74 ± 1.12 | + 112.5 |
| ***Il-1β*** | 22.56 ± 9.96 | 10.57 ± 2.58 | - 53.2 |
| ***Ly6g*** | 4.85 ± 2.66 | 1.31 ± 0.35 | - 73.0 |
| ***Ptsg2*** | 21.05 ± 10.78 | 6.35 ± 2.06 | - 69.9 |

**Supplemental Table 1. Comparative relative expression of inflammatory genes in murine arthritic joint tissue.** Arthritic mouse paws were collected for gene analysis on day 8 (see methods for details). Relative expression values were calculated following normalization to endogenous housekeeping gene *Rpl32* and using the $2^{-(\Delta\Delta Ct)}$ method normalized to a naïve mouse (calibrator sample).